Carbon 110 (2016) 330–335

Contents lists available at ScienceDirect

Carbon

journal homepage: www.elsevier.com/locate/carbon

Lattice distortion and electron charge redistribution induced by defects in graphene

Wei Zhang [a, b, **], Wen-Cai Lu [a, c], Hong-Xing Zhang [a], K.M. Ho [b], C.Z. Wang [b, *]

[a] International Joint Research Laboratory of Nano-Micro Architecture Chemistry and Institute of Theoretical Chemistry, Jilin University, Changchun, Jilin 130023, People's Republic of China
[b] Ames Laboratory, U.S. DOE and Department of Physics and Astronomy, Iowa State University, Ames, IA 50011, USA
[c] Department of Physics and State Key Laboratory Cultivation Base of Advanced Fibers and Textile Materials, Qingdao University, Qingdao, Shandong 266071, People's Republic of China

ARTICLE INFO

Article history:
Received 15 June 2016
Received in revised form
20 August 2016
Accepted 14 September 2016
Available online 14 September 2016

ABSTRACT

Lattice distortion and electronic charge localization induced by vacancy and embedded-atom defects in graphene were studied by tight-binding (TB) calculations using the recently developed three-center TB potential model. We showed that the formation energies of the defects are strongly correlated with the number of dangling bonds and number of embedded atoms, as well as the magnitude of the graphene lattice distortion induced by the defects. We also showed that the defects introduce localized electronic states in the graphene which would affect the electron transport properties of graphene.

1. Introduction

Graphene has appeared as one of the most remarkable new materials of the past 10 years due to its distinctive electronic, mechanical, and thermal properties [1–3]. However, mechanical strains induced by defects often give rise to surprising changes in the physical and chemical properties of graphene [4]. In recent years, novel physical properties in graphene induced by mechanical strain has been studied both experimentally [5–8] and theoretically [1,9,10]. Uniaxial strain can be induced in graphene by bending the substrates on which graphene is elongated [11]. Craco et al. unveil hidden electronic properties of isotropically strained graphene [12]. Jain et al. simulated buckling caused by strong long-range relaxations of typical defects such as the Stone–Wales (SW) defect in graphene [13]. The critical strain at which formation of SW defects in graphene becomes thermodynamically favorable was calculated to be 6–9% [14–16] and 12–17% [14,16], when the strain is applied in the zigzag and armchair directions, respectively. The geometry of stable dislocations also depends critically on whether they are formed from adatoms or vacancies [17,18]. Structure and deformation of the monovacancy near the edge of the graphene layer have been often observed by experiments [19,20] and have been studied by theoretical calculations [21]. Gong et al. showed that bond rotations at the edge of graphene can help to reduce the overall strain in the system [22]. Chen et al. show that bond rotations reduce the maximum single bond strain reached within a divacancy (DV) and help distribute the strain over a larger number of bonds to minimize the peak magnitude [23].

Understanding how defects deform graphene helps build an accurate description of both elasticity and plasticity in graphene [24–26]. While many theoretical and experimental studies have been devoted to elucidating the Stone–Wales (SW) defect structures and their electronic properties, much less studies have provided systematic evidence to connect other vacancy and embedded-atom defect structures with their lattice distortion and local electronic properties. In this paper, we performed a systematic calculation to study the lattice distortion and electronic charge variation caused by various vacancy and embedded-atom defects in graphene, in order to gain more comprehensive and deeper understanding of the properties of graphene subjected to point defects.

* Corresponding author.
** Corresponding author. International Joint Research Laboratory of Nano-Micro Architecture Chemistry and Institute of Theoretical Chemistry, Jilin University, Changchun, Jilin 130023, People's Republic of China.
E-mail addresses: zhangw_bxx@jlu.edu.cn (W. Zhang), wangcz@ameslab.gov (C.Z. Wang).

http://dx.doi.org/10.1016/j.carbon.2016.09.031
0008-6223/

2. Calculation methods

The calculations are performed using the three-center tight-binding potential recently developed [27]. The interatomic interactions in TB method are based on quantum mechanics descriptions thus has better accuracy than empirical classical potential can offer. At the same time, it can provide faster computing speed in comparison with first-principles methods such as density functional theory (DFT) because it use minimal basis and the hopping and overlap integrals are parametrized. It has been demonstrated that the newly developed three-center TB potential for carbon exhibits excellent accuracy and transferability. It describes well the band structures, binding energies and other properties of various carbon crystalline structures and surfaces. It is also very efficient for large scale atomistic simulations and can accurately describe the structures and energies of various defects in graphene. Details of TB methods have been described in previous literature [27]. The calculations presented in this paper were performed using a rectangular graphene supercell containing 1000 atoms and with a vacuum region of 50 Å in the direction perpendicular to the graphene and with periodic boundary conditions. The defect structures are fully relaxed until the forces on every atom are less than 0.01 eV/Å.

Our calculations are based on the most stable vacancy and adatom defects structures in graphene obtained from our calculations as well as those in the literature [28,29]. These structures are shown in Fig. 1. The simplest defects in graphene is the Stone Wales (SW) defect where four hexagons are transformed into two pentagons and two heptagons (i.e., 55—77 defect) by rotating one of the C—C bonds by 90°. Single vacancy (SV) in graphene prefers a five-membered and a nine-membered ring (i.e., a 5—9 defect). The stable structures of divacancy defect in graphene is the three-pentagons and three-heptagons V_2 (555—777) [28]. The lowest energy structure of trivacancy defect is composed of two five-membered and one ten-membered (heart-shape) rings, i.e., V_3 (5-10-5) which has one dangling bond. The V_4 (5555-66-7777) is the most favorable structure of tetravacancy defect which has six pentagons, six heptagons and two hexagons [29]. The stable structure of hexvacancy defect V_6 is obtained by removing a hexagonal ring from the graphene. The most stable structure for embedding two atoms contains a pair of joined pentagonal carbon rings placed between a pair of heptagonal rings, i.e., a A_2 (7-55-7) structure. Finally, the lowest-energy structure for embedding four atoms consist a core of a pair of adjacent five-membered rings, a hexagonal ring and another five-membered ring, surrounded by three seven-membered rings. We call this defect a A_4 (55-6-5-777) defect.

3. Results and discussions

3.1. Lattice distortion induced by defects in graphene

Defects in graphene can induce significant distortions to the graphene lattice. Such distortions can spread far away from the defects because most of the distortions are elastic in nature. Since TB calculation can handle a large number of atoms, it is very useful for studying the structure distortion caused by the defects in graphene. In Fig. 2, we show the bond length variation in the defect structures with respect to the equilibrium bond length (1.42 Å) in perfect graphene. Larger lattice distortions can be well seen at the vicinity of the defects, some bonds are stretched (brown or red) and some are compressed (blue or purple) which can also be seen clearly in Fig. 2. Away from the defects, the distortions become smaller but can extend to large distance from the center of the defect, particularly for SW, and V_2-V_4 defects. For these defects, the bonds are found to be compressed in some directions (cyan) and stretched in other directions (light green). The lattice distortion in SV and V_6 are more localized due to the formation of the dangling bonds around the vacancy. In addition to the in-plane distortion, the SW, A_2, and A_4 defects also have significant vertical distortion as one can see from Fig. 2. In particular, the SW exhibits vertical cosine distortions with buckling heights of 2.10. The formation of the bulge along the z-direction in A_2 and A_4 structures also help

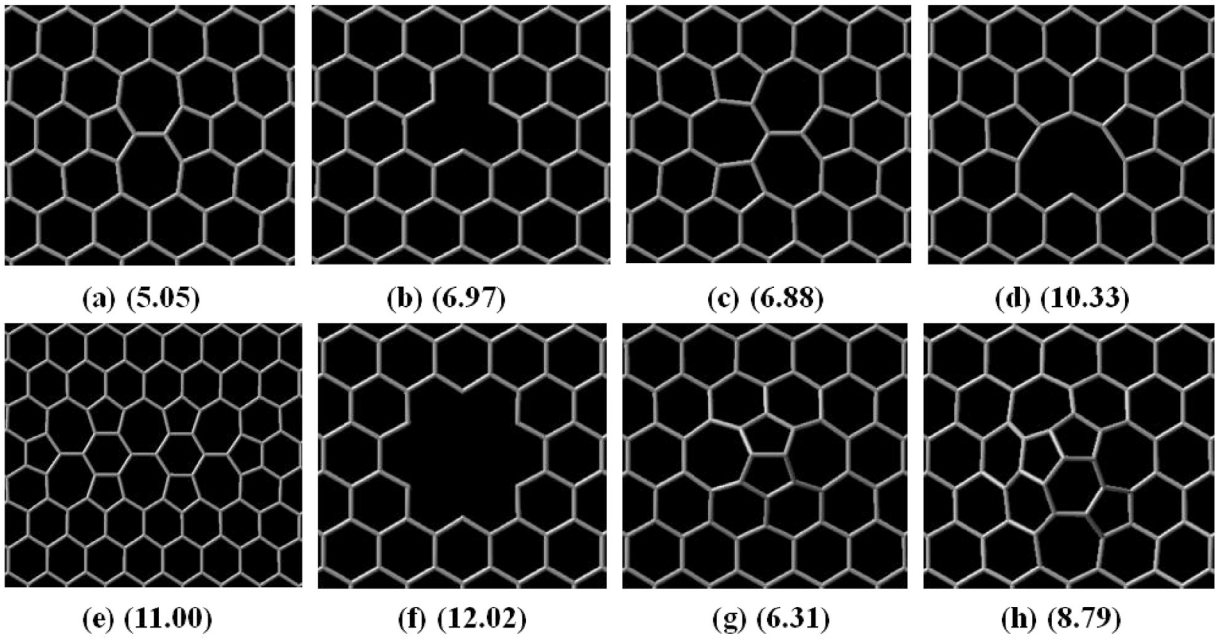

Fig. 1. The lowest-energy structures and formation energies (in eV shown in the parenthesis) of (a) SW(55-77), (b) SV(5-9), (c) V_2 (555-777), (d) V_3 (5-10-5), (e) V_4 (5555-66-7777), (f) V_6, (g) A_2 (7-55-7), and (h) A_4 (55-6-5-777) defects calculated by the 3-center TB.